

# Phosphorylation of signal transducer and activator of transcription 1 reduces bortezomib-mediated apoptosis in cancer cells

C Kao<sup>1,2,6</sup>, A Chao<sup>\*,1,6</sup>, CL Tsai<sup>1</sup>, CY Lin<sup>1</sup>, WC Chuang<sup>1,2</sup>, HW Chen<sup>1,2</sup>, TC Yen<sup>3</sup>, TH Wang<sup>\*,1,2,4</sup>, CH Lai<sup>1</sup> and HS Wang<sup>1,5</sup>

The potent and selective proteasome inhibitor bortezomib has shown remarkable antitumor activity and is now entering clinical trials for several cancers. However, the molecular mechanisms by which bortezomib induces cytotoxicity in ovarian cancer cells still remain unclear. In this study, we show that bortezomib induced apoptosis, which was demonstrated by the downregulation of antiapoptotic molecules (Bcl-2, Bcl-XL, p-Bad, and p-AKT) and the upregulation of proapoptotic proteins (p21, p27, and cleaved-Bid) in ovarian cancer cell lines. Moreover, bortezomib stimulates Janus kinase (JAK) phosphorylation and activates heat-shock transcription factor-1 (HSF-1) and heat-shock protein 70 (HSP70), ultimately leading to signal transducer and activator of transcription 1 (STAT1) phosphorylation. Phosphorylated STAT1 partially counteracted apoptosis induced by bortezomib in cancer cells. These findings suggest that the antitumor activity of bortezomib in ovarian cancer can be improved by inhibiting bortezomib-induced STAT1 phosphorylation. This effect can be achieved by STAT1 knockdown, HSP70 knockdown, JAK inhibition, or the addition of cisplatin, one of the most commonly used anticancer drugs. These results provide the first evidence that STAT1 phosphorylation can play a role in bortezomib resistance by exerting antiapoptotic effects. They also suggest the possibility to abolish or reduce bortezomib chemoresistance in ovarian cancer by the addition of cisplatin or JAK inhibitors.

*Cell Death and Disease* (2013) 4, e512; doi:10.1038/cddis.2013.38; published online 28 February 2013

**Subject Category:** Cancer

The potent and selective proteasome inhibitor bortezomib (Velcade, formerly known as PS-341) has shown remarkable antitumor activity and is currently approved for the treatment of multiple myeloma (MM).<sup>1</sup> Growing evidence suggests that bortezomib induces tumor cell apoptosis and inhibits tumor growth.<sup>1–3</sup> In addition to its general mechanism through proteasome inhibition,<sup>4</sup> one of the antimyeloma mechanisms of bortezomib is the inhibition of the transcription factor nuclear factor- $\kappa$ B (NF- $\kappa$ B).<sup>4</sup> NF- $\kappa$ B has been shown to be constitutively activated in several types of cancer cells, and blockade of NF- $\kappa$ B has been reported to increase the cellular susceptibility to apoptosis.<sup>5</sup> The combination of bortezomib, melphalan,<sup>6</sup> or thalidomide<sup>7</sup> has been successfully used to treat patients with relapsed/refractory MM.

Signal transducer and activator of transcription 1 (STAT1), a member of a family of latent cytoplasmic transcription factors, has a crucial role in a variety of biological functions, including cell proliferation and apoptosis.<sup>8,9</sup> It has been

demonstrated that interferons or interleukins can activate Janus kinase (JAK) and Tyk2, which is followed by tyrosine phosphorylation of different STAT family members (STAT1, STAT2, and STAT3).<sup>9</sup> STAT1 can also block mdm2, a molecule that inhibits p53 transcriptional activity and stimulates its degradation. The cleavage of STAT1 by caspase-3 releases a C-terminal peptide, which interacts with p53 to induce apoptosis. Once released, the proapoptotic C-terminal fragment of STAT1 may further stimulate caspase activity, resulting in a self-perpetuating activation loop. Moreover, STAT1-induced apoptosis is, in part, mediated by caspase-2 and -7.<sup>8</sup> Evidence also suggests that activated STAT1 may regulate apoptosis by enhancing the transcription of procaspase-8, Bax, Bcl-2, and Bcl-X.<sup>10</sup> STAT1 phosphorylated at serine 727 and tyrosine 701 can induce apoptotic cell death in heart, brain, and liver tissues following ischemia–reperfusion injury. In addition, it has been demonstrated that both serine 727 and tyrosine 701 of STAT1 are

<sup>1</sup>Department of Obstetrics and Gynecology, Linkou Medical Center, Chang Gung Memorial Hospital, Chang Gung University, Taoyuan, Taiwan 333, Republic of China;

<sup>2</sup>Graduate Institute of Biomedical Sciences, College of Medicine, Chang Gung University, Taoyuan, Taiwan 333, Republic of China; <sup>3</sup>Department of Nuclear Medicine, Linkou Medical Center, Chang Gung Memorial Hospital, Taoyuan, Taiwan 333, Republic of China; <sup>4</sup>Genomic Medicine Research Core Laboratory, Linkou Medical Center, Chang Gung Memorial Hospital, Taoyuan, Taiwan 333, Republic of China and <sup>5</sup>Graduate Institute of Clinical Medical Sciences, College of Medicine, Chang Gung University, Taoyuan, Taiwan 333, Republic of China

\*Corresponding author: A Chao or TH Wang, Department of Obstetrics and Gynecology, Linkou Medical Center, Chang Gung Memorial Hospital, Chang Gung University, No. 5, Fushin Street, Guishan, Taoyuan, Taiwan 333, Republic of China. Tel: +886 3 3281200 ext. 5402; Fax: +886 3 3288252;

E-mail: angel945@cgmh.org.tw or knoxtn@cgmh.org.tw

<sup>6</sup>These authors contributed equally to this work.

**Keywords:** bortezomib; ovarian cancer; cisplatin; HSP70; JAK1; STAT1

**Abbreviations:** BTZ, bortezomib; CDDP, cisplatin; HSF-1, heat-shock transcription factor-1; HSP70, heat-shock protein 70; JAK1, Janus kinase 1; JAKi, JAK inhibitor; STAT1, signal transducer and activator of transcription 1

Received 05.11.12; revised 15.1.13; accepted 16.1.13; Edited by A Stephanou

phosphorylated in response to JAK and p38 activation in Streptococcal pyrogenic exotoxin B-induced apoptosis.<sup>10</sup> Although the proapoptotic effects of STAT1 have been widely reported, only a few studies have focused on its potential antiapoptotic properties.<sup>11,12</sup>

Ovarian cancer is the leading cause of death from gynecological cancer.<sup>13</sup> Patients with ovarian cancer have 5-year survival rates that range from 36 to 44%, depending on the stage.<sup>13</sup> The standard treatment is surgery, usually combined with adjuvant chemotherapy. Although combination regimens of paclitaxel and the platinum drugs are considered as a first-line treatment option for ovarian cancer,<sup>14</sup> the majority of women with advanced ovarian malignancies will ultimately relapse and develop drug-resistant disease (median progression-free survival: 18 months).<sup>15</sup> Thus, there is an urgent need for the development of more effective treatment modalities that could improve the prognosis.

Ovarian cancer cells are characterized by high levels of proteasome activity and increased accumulation of ubiquitinated proteins; consistent with this, they are sensitive to apoptosis induced by proteasome inhibitors.<sup>16</sup> The proteasome inhibitor bortezomib is now entering clinical trials for ovarian cancer. In a phase I study, the combination of bortezomib and carboplatin elicited an overall response rate of 47% in recurrent ovarian or primary peritoneal cancer.<sup>17</sup> Notably, bortezomib has been shown to induce ovarian cancer cell death by decreasing the levels of Bcl-XL and X-linked inhibitor of apoptosis protein.<sup>18</sup> In addition, bortezomib has the ability to promote cell cycle arrest and apoptosis through the induction of p21/p27 and the activation of caspase-3.<sup>16</sup> Despite these promising results, a Gynecologic Oncology Group phase II trial has reported that bortezomib has minimal activity as a single agent in the treatment of recurrent platinum-sensitive epithelial ovarian or primary peritoneal cancer.<sup>19</sup> Importantly, the molecular mechanisms underlying the antineoplastic effects of bortezomib (either alone or in combination with other drugs) have not yet been completely elucidated.

In this study, we sought to identify the signaling cascades leading to bortezomib-triggered cell death. Signaling pathways were investigated using 11 reporter assays. Our data indicate that STAT1 phosphorylation (which exerts an antiapoptotic activity) may partly explain why bortezomib monotherapy showed limited antitumor activity in ovarian cancer patients in the phase II trial. We also demonstrate that bortezomib-activated STAT1 phosphorylation may be suppressed with the combined use of bortezomib with either JAK inhibitors (JAKi's) or cisplatin, one of the most commonly used anticancer drugs.

## Results

**Bortezomib induces cancer cell death and activates the STAT1 signaling pathway.** In all, 10 ovarian cancer cell lines, including serous (OV90, 67R, BG1, BR, SKOV3, and OVCAR3), endometrioid (TOV112D and MDAH2774), and clear-cell (TOV21G and ES2) carcinomas were exposed to bortezomib (Figure 1a). TOV112D, OVCAR3, and TOV21G cells demonstrated the highest sensitivity to bortezomib (mean effective concentration ( $EC_{50}$ ): 0.05–0.1  $\mu$ M). ES2,

BG1, OV90, and MDAH2774 cells showed an intermediate sensitivity to bortezomib (mean  $EC_{50}$ : 1–10  $\mu$ M), whereas 67R, BR, and SKOV3 cells had the highest bortezomib resistance. Bortezomib induced a higher cytotoxicity in the TOV112D and TOV21G cells than in BR and SKOV3 cells, respectively (Figure 1b). In general, bortezomib promoted caspase-3 activation in a dose-dependent manner, despite significant differences in terms of sensitivity (high in TOV112D and TOV21G cells, and low in BR and SKOV3 cells; Figure 1c). Bortezomib induced apoptosis, which was shown by the upregulation of both proapoptotic proteins p21 and p27 (resulting in an arrest of the cell cycle), increased apoptotic markers (cleaved-PARP and cytochrome *c* release), and the downregulation of antiapoptotic proteins (Bcl-2, Bcl-XL, and p-Bad; Figure 1d).

Signaling pathways induced by bortezomib were investigated using 11 reporter assays in TOV112D cells. Bortezomib reduced the activity of the HRE (hypoxia response element), NPM1/B23, E2F1, MMP9, and YY1 reporters (Supplementary Figure 1a). In contrast, bortezomib significantly activated the C/EBP, Grp78, ID3, STAT1, and TOP reporters. Surprisingly, bortezomib did not induce a significant activation of the NF- $\kappa$ B reporter (Figure 1e). The JAK/STAT signaling pathway was specifically activated by bortezomib, but neither by another proteasome inhibitor (MG132) nor by paclitaxel (Figure 1f and Supplementary Figure 1b). In accordance with the results of the reporter assay, bortezomib was found to activate STAT1 phosphorylation in TOV112D, TOV21G, BR, and SKOV3 cells. STAT1 phosphorylation levels were inversely correlated with the sensitivity to bortezomib (Figure 1g).

**The inhibition of JAK1/STAT1 signaling pathway sensitizes ovarian cancer cells to bortezomib-mediated cytotoxicity.** RNAi-mediated STAT1 knockdown suppressed the expression of both total and phosphorylated STAT1 (Figure 2a). Although the knockdown of STAT1 alone did not induce caspase-3 activation, the suppression of STAT1 phosphorylation significantly increased bortezomib-induced apoptosis (Figure 2b). JAK1 is a known regulator of STAT1, and JAKi I suppressed bortezomib-induced phosphorylation of both STAT1 (Figure 2c) and JAK1 (Figure 2d). The inhibition of JAK significantly increased bortezomib-mediated caspase-3 activation (Figure 2e). The combination of bortezomib and JAKi I resulted in higher cytotoxic effects than when cells were exposed to either JAKi I or bortezomib alone (Figure 2f). Similar results were observed in TOV21G, BR, and SKOV3 cells, suggesting that the inhibition of STAT1 phosphorylation can sensitize ovarian cancer cells to bortezomib (Figure 2g). Overexpression of an S727E-substituted STAT1, which mimicked the S727-phosphorylated STAT1, counteracted cell death that was induced by either bortezomib alone or combined bortezomib with JAKi (Figure 2h and Supplementary Figure 5).

**The effects of HSP70 on STAT1 in bortezomib-mediated cytotoxicity are transcriptionally activated by heat-shock factor-1.** Because bortezomib can induce heat-shock protein (HSP)-related stress,<sup>20</sup> we sought to investigate the potential role played by HSP70 in the

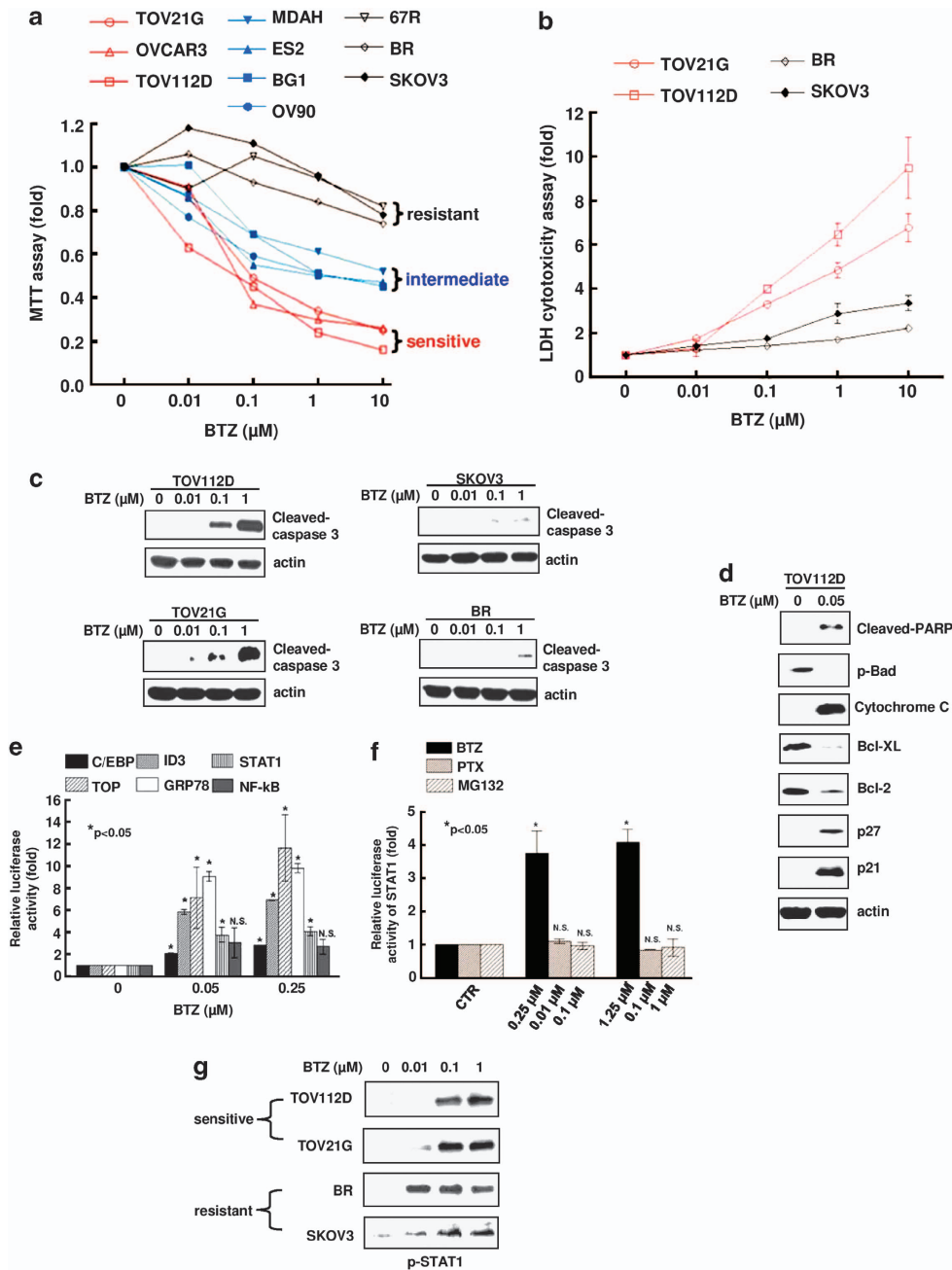


**Figure 1** Bortezomib (BTZ) induces dose-dependent inhibition or activation of specific reporter assays in ovarian cancer cells. (a) Ovarian cancer cell lines (SKOV-3, ES-2, TOV-21G, TOV112D, OV90, 67R, BG1, OVCAR3, MDAH, and BR) were treated with either the vehicle alone or BTZ (concentration range: 0.01 – 10  $\mu\text{M}$ ) for 48 h. The MTT assay was used to determine the cell viability. (b) The cytotoxic effects of BTZ (duration of exposure: 24 h) were determined using the LDH assay in the TOV112D, TOV21G, BR, and SKOV3 cancer cell lines. (c) BTZ induced a dose-dependent activation of caspase-3 in TOV112D, TOV21G, BR, and SKOV3 cells. (d) The effects of BTZ (concentration: 0.05  $\mu\text{M}$ ; duration of exposure: 24 h) in TOV112D cells were investigated by immunoblotting; specifically, the protein levels of antiapoptotic (Bcl-2, Bcl-XL, and p-Bad) and proapoptotic (PARP, cleaved-caspase-3, cytochrome c, and p21/p27) molecules were determined. (e) TOV112D cells were transfected using the indicated reporter constructs, and subsequently treated with 0.05 or 0.25  $\mu\text{M}$  of BTZ for 24 h. The activation of the specific gene promoters (Grp78, ID3) and the consensus response elements (C/EBP, STAT1, TOP-flash, NF- $\kappa\text{B}$ ) was determined using the luciferase activity assay. (f) TOV112D cells were transfected with the STAT1 response element construct and treated with BTZ, paclitaxel, and MG132 at the indicated concentrations for 24 h. The STAT1 activity was measured using the luciferase assay. (g) The effects of 0.01–1  $\mu\text{M}$  of BTZ (duration of exposure: 24 h) on the activation of STAT1 phosphorylation in TOV112D, TOV21G, BR, and SKOV3 cells were determined by immunoblotting. Data are expressed as mean  $\pm$  standard error of the mean. The results are representative of at least three independent experiments

cytotoxic effects of bortezomib in ovarian cancer cells. In TOV112D cells, bortezomib significantly upregulated HSP70 expression both at the transcriptional (mRNA) and protein levels (Figure 3a); similar findings were observed in four

other ovarian cancer cell lines (Supplementary Figures 2a–d). RNAi-mediated HSP70 knockdown increased the activation of caspase-3 and the cytotoxic effects of bortezomib in TOV112D cells (Figures 3b and c). Similar results

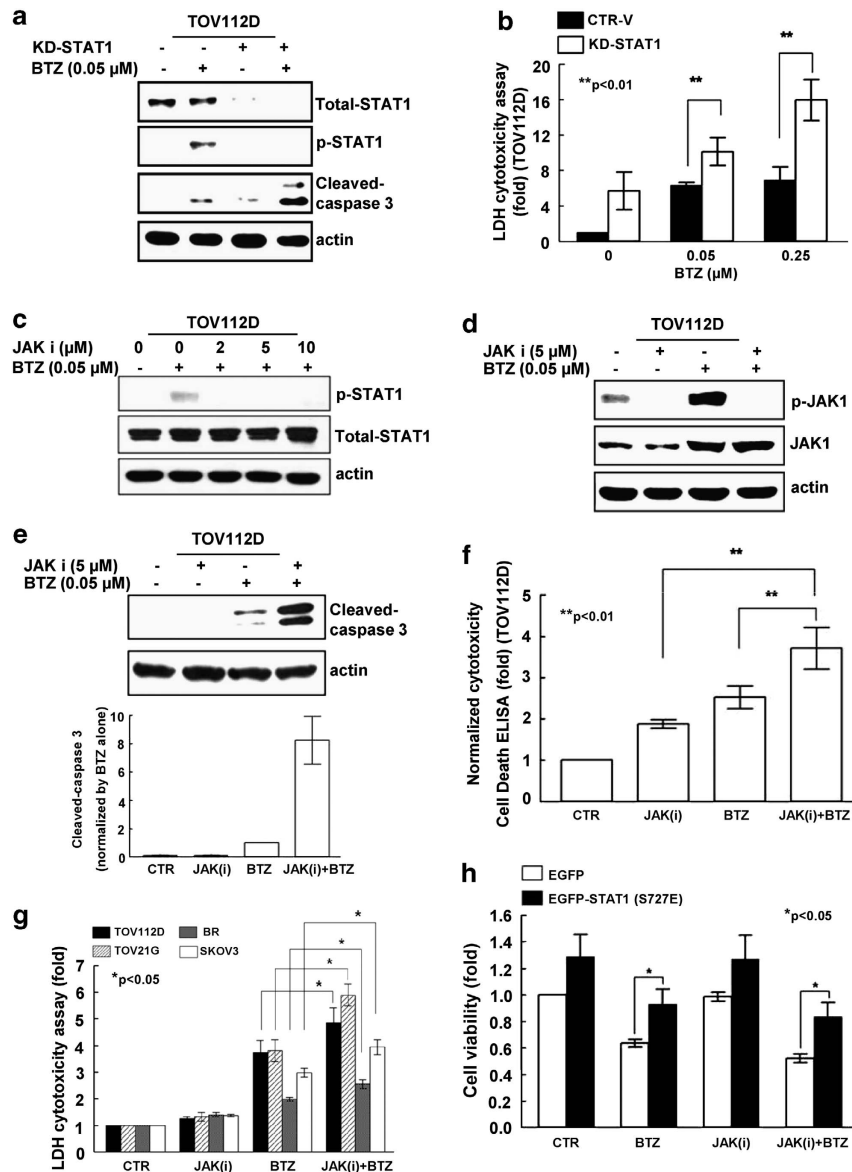


**Figure 2** The suppression of STAT1 and JAK enhances bortezomib (BTZ)-induced cancer cells' death. (a and b) The knockdown of STAT1 by short hairpin (sh)RNA and the treatment with 0.05  $\mu$ M of BTZ for 24 h in TOV112D cells were analyzed by immunoblotting; specifically, the levels of caspase-3 cleavage were measured. Cytotoxicity was measured using the LDH assay. (c) Inhibition of the JAK/STAT pathway with JAKi. (d) TOV112D cells were treated with 5  $\mu$ M of JAKi and 0.05  $\mu$ M of BTZ for 24 h. Cell lysates were analyzed by immunoblotting to determine the levels of phosphorylated JAK1 and JAK1. (e) TOV112D cells treated with 0.05  $\mu$ M of BTZ and 5  $\mu$ M of JAKi for 24 h were analyzed by immunoblotting to determine the levels of caspase-3 cleavage. (f) The cytotoxicity of the combined treatment with JAKi and BTZ was measured using the Cell Death Detection ELISA in TOV112D cells. (g) LDH assays were used for the TOV112D, TOV21G, BR, and SKOV3 cells. (h) TOV112D cells were transiently transfected with enhanced green fluorescent protein (EGFP) alone (control vector) or EGFP-STAT1 (S727E) for 72 h, and then treated with 5  $\mu$ M of JAKi and 0.05  $\mu$ M of BTZ for 24 h. Cell viability was analyzed using the MTT assay. Data are expressed as mean  $\pm$  standard error of the mean. The results are representative of at least three independent experiments

were obtained in MDAH2774 cells (Supplementary Figures 2e and f). Of note, the suppression of HSP70 resulted in a significant inhibition of bortezomib-induced STAT1 phosphorylation (Figure 3d). Moreover, overexpression of HSP70 significantly increased the phosphorylation of STAT1 and further enhanced bortezomib-induced phosphorylation of STAT1 (Figure 3e), and also rescued bortezomib-mediated cell death (Figure 3f). Bortezomib significantly activated the heat-shock factor (HSF) response element reporter (Figure 3g) and increased HSF-1 protein levels

(Supplementary Figure 3a). The knockdown of HSF-1 with shRNA (Supplementary Figure 3b) decreased HSP70 protein levels and increased caspase-3 activation (Figure 3h). In line with these results, the overexpression of either HSF-1 or HSP70 significantly reduced bortezomib-induced caspase-3 activation (Supplementary Figure 3c). Collectively, these results demonstrate that the HSF1–HSP70–STAT1 signaling pathway is involved in cell survival, counteracting the cytotoxicity of bortezomib.

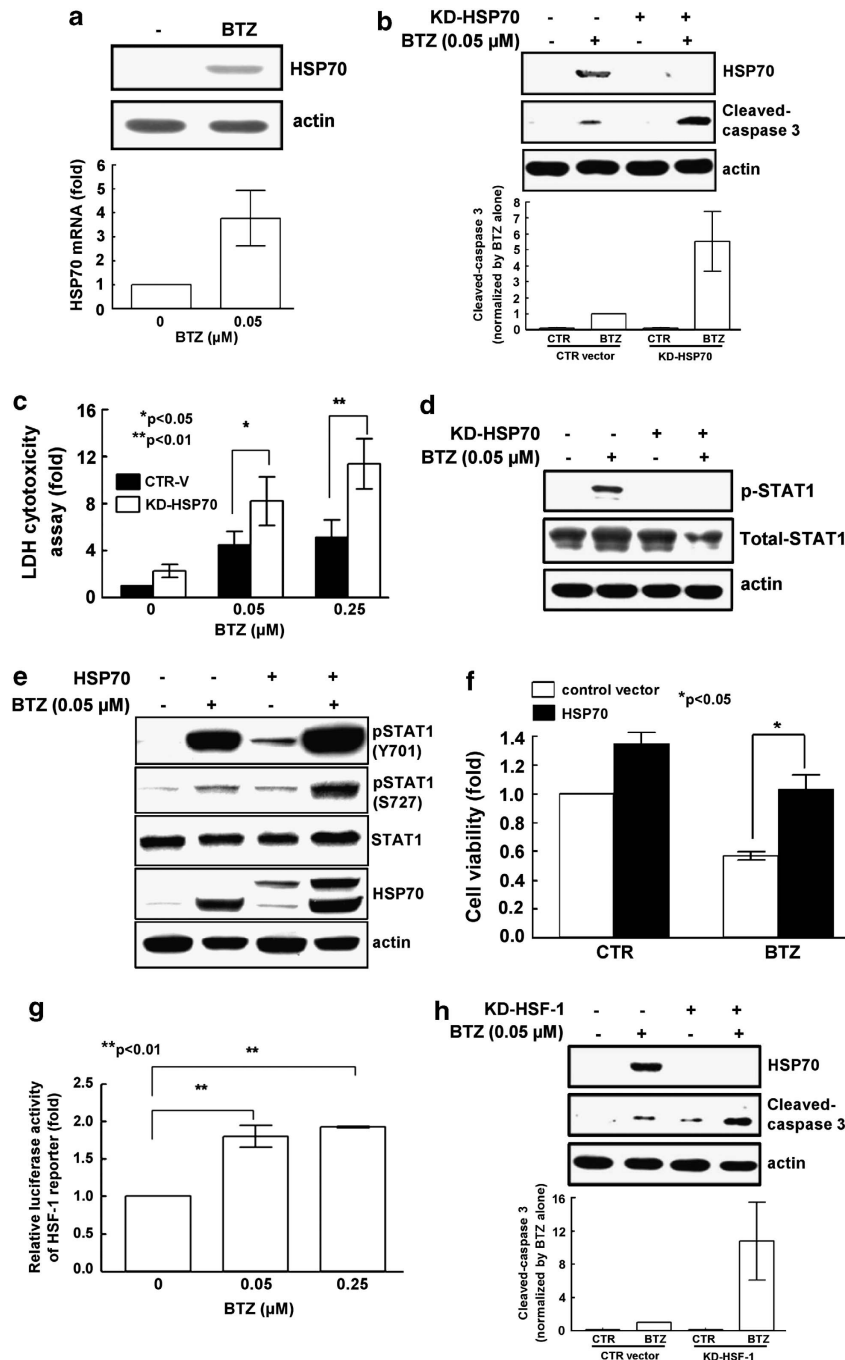


**Figure 3** The HSF-1–HSP70–STAT1 signaling pathway is involved in bortezomib (BTZ)-induced cytotoxicity. (a) TOV112D cells were treated with 0.05  $\mu$ M of BTZ for 24 h. HSP70 mRNA and protein levels were measured by real-time quantitative PCR and western blot analysis, respectively. (b) The effects of the HSP70 knockdown by short hairpin (sh)RNA and the treatment with 0.05  $\mu$ M of BTZ for 24 h in TOV112D cells were analyzed by measuring the levels of caspase-3 cleavage and (c) using the LDH assay. For clarity of presentation, data were normalized with that of BTZ-treated cells, which was set as 1. (d) The effects of the HSP70 knockdown by shRNA on the regulation of STAT1 phosphorylation in BTZ-treated TOV112D cells were determined by immunoblotting. (e) Treatment with BTZ stimulated phosphorylation of STAT1 at tyrosine 701 and serine 727, which was enhanced by overexpression of HSP70. (f) The overexpression of HSP70 attenuated BTZ-mediated growth inhibition. Cell viability was analyzed using the MTT assay. (g) TOV112D cells were transfected with an HSE reporter construct. The dose-dependent activation of HSF-1 was measured using luciferase assays after 24 h of treatment with BTZ. (h) TOV112D cells were treated with 0.05  $\mu$ M of BTZ for 24 h, and the effects of HSF-1 knockdown on the regulation of HSP70 and caspase-3 cleavage were analyzed by immunoblotting. For clarity of presentation, data were normalized with that of BTZ-treated cells, which was set as 1. Data are expressed as mean  $\pm$  standard error of the mean. The results are representative of at least three independent experiments

**STAT1 attenuates bortezomib-induced apoptosis.** Bortezomib triggered apoptosis, shown by downregulation of the antiapoptotic proteins Bcl-2, Bcl-XL, and p-Bad (Figure 1d).

The knockdown of STAT1 further suppressed the antiapoptotic molecules Bcl-2, Bcl-XL, and p-Bad (Figures 4a, b and d, e), and increased the levels of cleaved-Bid (Figures 4a

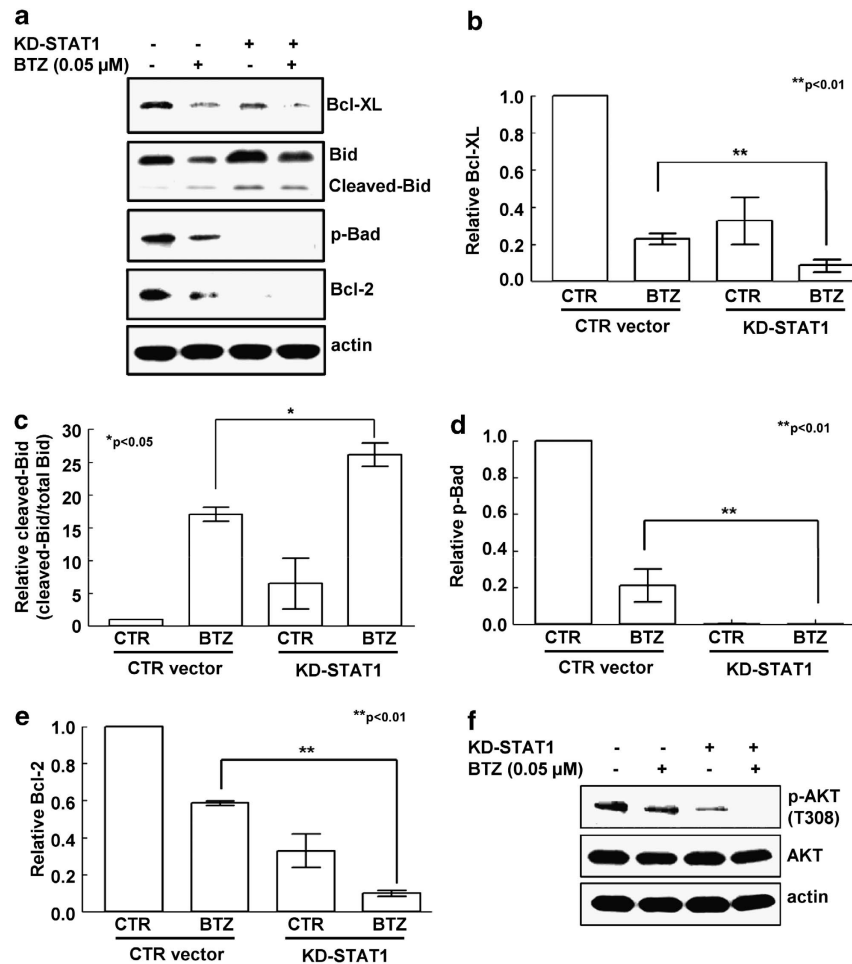


**Figure 4** The knockdown of STAT1 promotes bortezomib (BTZ)-induced apoptosis in ovarian cancer cells. (a) The effects induced by the treatment with BTZ (0.05  $\mu$ M for 24 h) and the knockdown of STAT1 by short hairpin (sh)RNA on TOV112D cancer cells were analyzed in TOV112D cells using immunoblotting; specifically, the levels of the antiapoptotic proteins (Bcl-2, Bcl-XL, and p-Bad,) and the cleavage of Bid were determined. The quantitative data obtained for these proteins are presented in panels b–e. (f) TOV112D cells were exposed to a combination of BTZ (0.05  $\mu$ M) and STAT1 shRNA for 24 h and then analyzed by immunoblotting for AKT phosphorylation (T308). Data are expressed as mean  $\pm$  standard error of the mean. The results are representative of at least three independent experiments

and c) in bortezomib-treated TOV112D cancer cells. These results suggest that STAT1 may increase the cell viability in bortezomib-treated ovarian cancer cells by modulating several different molecules involved in the apoptotic cascade. Moreover, bortezomib inhibited AKT activity by suppressing the phosphorylation of AKT (T308). Similarly, the knockdown of STAT1 further decreased AKT phosphorylation (T308), which was already reduced by bortezomib (Figure 4f). Taken together, these results indicate that STAT1 has an antiapoptotic role in bortezomib-induced cytotoxicity in ovarian cancer cell lines.

**The combination of bortezomib and cisplatin decreases bortezomib-induced phosphorylation of STAT1 and enhances apoptosis.** Cisplatin, either alone or in combination with other agents, is the mainstay of chemotherapy in patients with ovarian cancer.<sup>21</sup> Platinum-based chemotherapy combined with bortezomib is now being investigated as a potential treatment for ovarian cancer.<sup>22</sup> However, the molecular mechanisms involved in the combination treatment with platinum-based agents and bortezomib have

not been fully elucidated. To this aim, ovarian cancer cells were exposed to bortezomib and cisplatin at a subcytotoxic concentration. Because the  $EC_{50}$  of cisplatin in TOV112D cells was approximately 50  $\mu$ M (Figure 5a), cisplatin was used at a final concentration of 5  $\mu$ M for the drug combination experiments. The combination of bortezomib and cisplatin significantly decreased cell viability to a greater degree than either agent alone (Figure 5b). Such a synergistic interaction was confirmed in the cytotoxicity assays (Figures 5c and d) and was also observed in bortezomib-resistant BR and SKOV3 cells (Supplementary Figures 4a and b). Moreover, cisplatin abolished bortezomib-induced phosphorylation of STAT1 (Figure 5e). The addition of cisplatin to bortezomib resulted in a significant increase in the cleavage of caspase-3 compared with bortezomib alone (Figure 5e). Taken together, these results indicate that cisplatin suppresses bortezomib-induced phosphorylation of STAT1 and enhances cytotoxicity by elevating apoptosis.

**Bortezomib induces cytotoxicity *in vivo*.** Luciferase-expressing mouse ovarian surface epithelial cancer cells

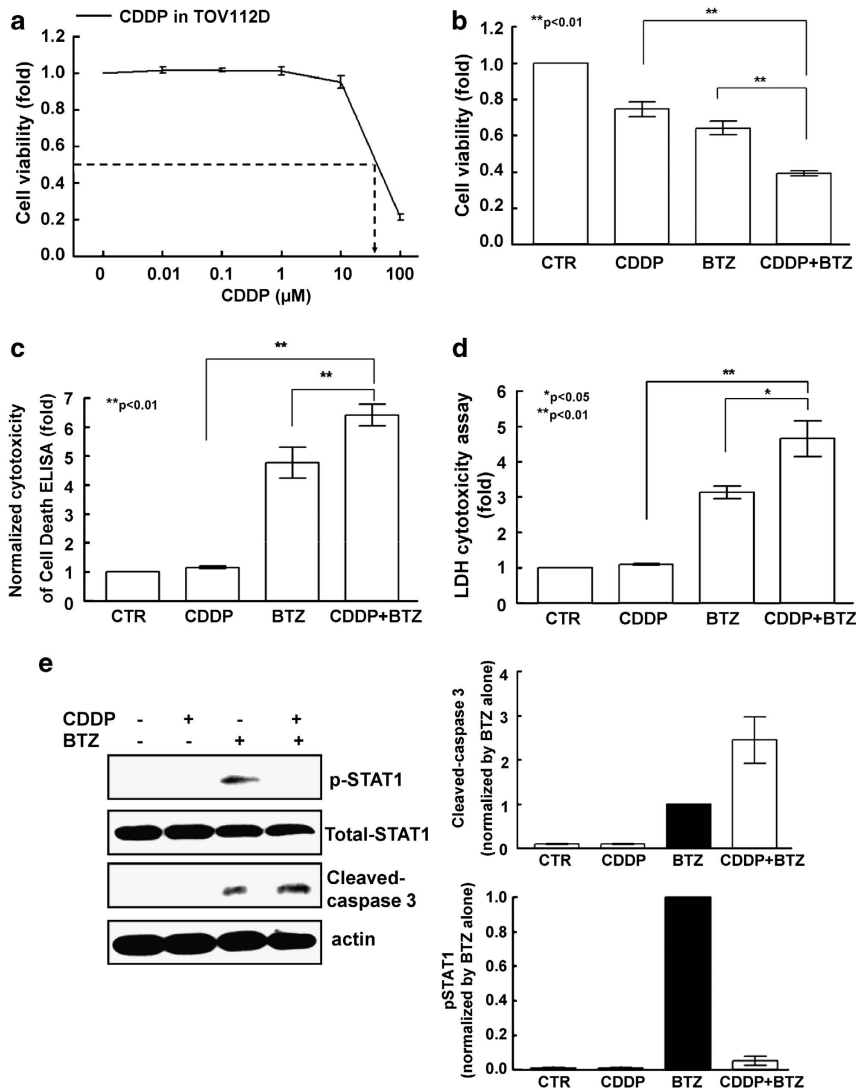


**Figure 5** Synergistic cytotoxic effects of the combination of cisplatin (CDDP) and bortezomib (BTZ) in ovarian cancer cells. (a) In the MTT assays, cancer cells were treated with CDDP at different concentrations for 24 h. The  $EC_{50}$  of CDDP was approximately  $50 \mu\text{M}$ . (b) TOV112D cells were treated with  $5 \mu\text{M}$  of CDDP and  $0.05 \mu\text{M}$  of BTZ for 24 h. Cell viability was assessed using the MTT assay. The cytotoxic effects caused by the combined treatment ( $5 \mu\text{M}$  of CDDP and  $0.05 \mu\text{M}$  of BTZ) were analyzed using (c) the Cell Death ELISA and (d) the LDH assays. (e) TOV112D cells were exposed to the combination of CDDP ( $5 \mu\text{M}$ ) and BTZ ( $0.05 \mu\text{M}$ ) for 24 h, and subsequently analyzed by immunoblotting for the levels of caspase-3 cleavage and STAT1 phosphorylation. For clarity of presentation, data were normalized with that of BTZ-treated cells, which was set as 1 (black bar). Data are expressed as mean  $\pm$  standard error of the mean. The results are representative of at least three independent experiments

(MOSEC/LUC) showed sensitivity to the treatment with bortezomib ( $EC_{50}$ :  $0.1 \mu\text{M}$ ; Figure 6a). Western blot analysis showed that phosphorylated STAT1, HSP70, and cleaved-caspase-3 were significantly increased in bortezomib-treated MOSEC/LUC cells (Figure 6b). We found evidence of an additional activation of bortezomib-induced caspase-3 when either JAKi 1 or AG490 were used to suppress phosphorylated JAK (Figures 6c and d). These results were consistent with those obtained using TOV112D cells (Figures 2e and f). Tumor growth was tracked by using the Xenogen IVIS 200 *In Vivo* Imaging System (Xenogen Corp., Alameda, CA, USA) to measure luciferase activity in MOSEC/LUC tumor-bearing C57BL/6 mice. The combination of bortezomib and AG490 inhibited tumor proliferation more effectively than bortezomib alone (Figures 6e and f). Moreover, the combination of bortezomib and AG490 was associated with

higher levels of cleaved-caspase-3 and lower levels of phosphorylated STAT1 in tumor tissues compared with bortezomib alone (Figure 6g). Collectively, these results support the potential usefulness of the combined treatment with bortezomib and JAKi's in ovarian cancer.

## Discussion

In this study, we systematically surveyed the signaling pathways regulated by bortezomib and demonstrated for the first time that the inhibition of STAT1 enhances bortezomib-induced cytotoxicity in ovarian cancer cells (Figure 7). Bortezomib is a proteasome inhibitor approved for clinical use in MM.<sup>7</sup> Here, we investigated the molecular mechanisms of bortezomib-induced cell death in ovarian cancer cells using a panel of 11 reporter assays examining different signaling

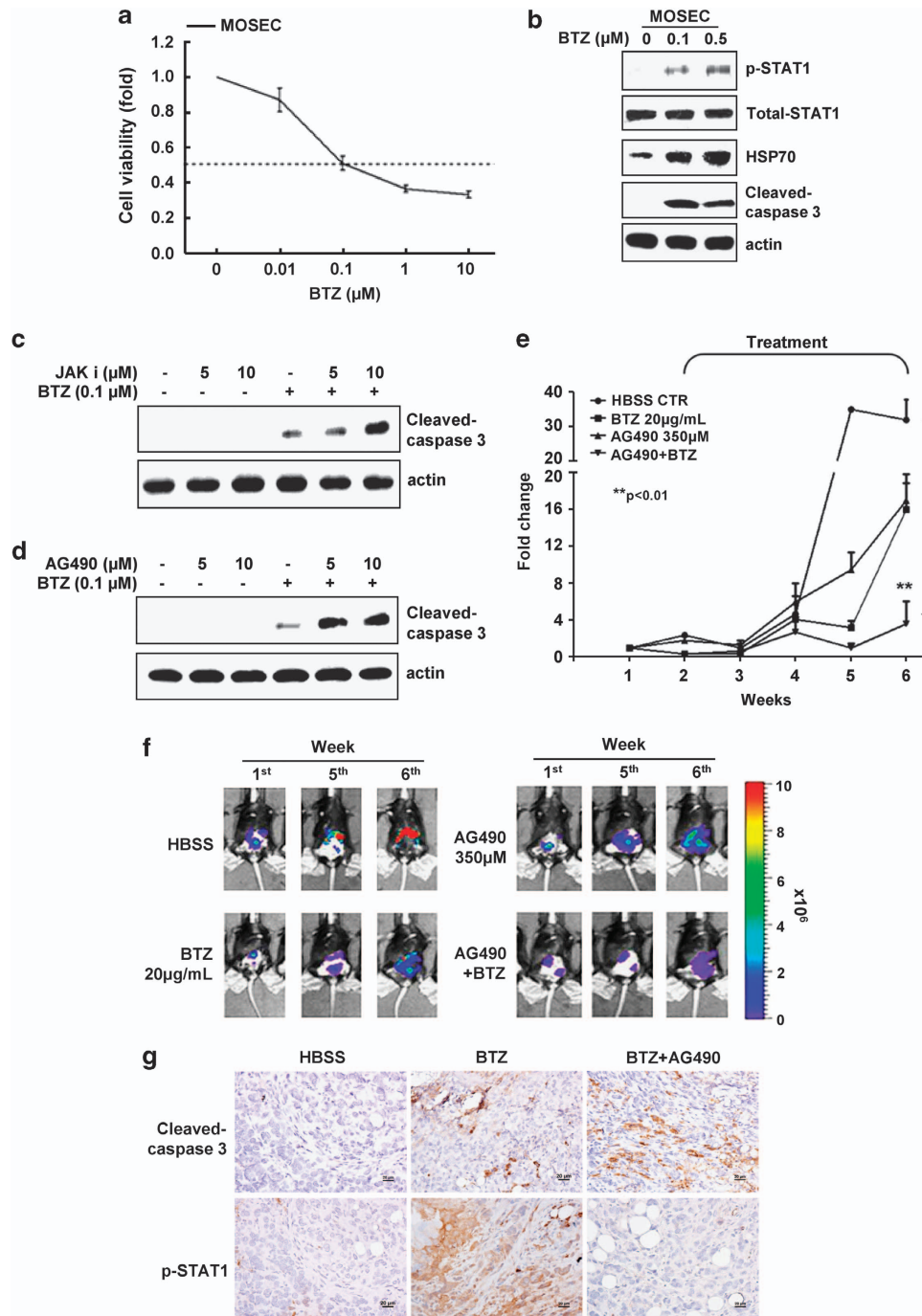


**Figure 6** Bortezomib (BTZ) inhibits ovarian cancer cell growth in mice. (a) Mouse ovarian surface epithelial cancer cells that constitutively expressed luciferase (MOSEC/LUC) were treated with BTZ at different concentrations (from 0.01 to 10  $\mu\text{M}$ ) for 48 h. Cell viability was measured with the MTT assay. (b) The effects of a 24-h exposure to BTZ (0.1 and 0.5  $\mu\text{M}$ ) were analyzed in MOSEC/LUC cells by immunoblotting; specifically, the levels of HSP70, phosphorylated STAT1, and cleaved-caspase-3 (c and d) were determined. The dose-dependent effects of JAKi I (AG490) on BTZ-induced cytotoxicity in MOSEC/LUC were measured by immunoblotting to determine the levels of cleaved-caspase-3. (e) Ten million MOSEC/LUC cells were intraperitoneally injected into C57BL/6 mice. Subsequently, the mice were intraperitoneally injected with 100  $\mu\text{l}$  of HBSS (vehicle alone), 20  $\mu\text{g/ml}$  of BTZ (for each mouse), 100  $\mu\text{l}$  of JAKi (AG490; concentration: 350  $\mu\text{M}$ ), or both BTZ and AG490 in combination three times a week. At 10 min after the intraperitoneal injection of luciferin, the mice were imaged using the IVIS 200 *in vivo* imaging system (f). Data are expressed as mean  $\pm$  standard error of the mean. The results are representative of at least three independent experiments. (g) Immunohistochemistry for phosphorylated STAT1 and cleaved-caspase-3 (brown color) in tumor sections obtained using the HBSS control (left), BTZ alone (middle), or the combination of BTZ with AG490 (right). Cell nuclei were counterstained with hematoxylin. Scale bars represent 20  $\mu\text{m}$ .



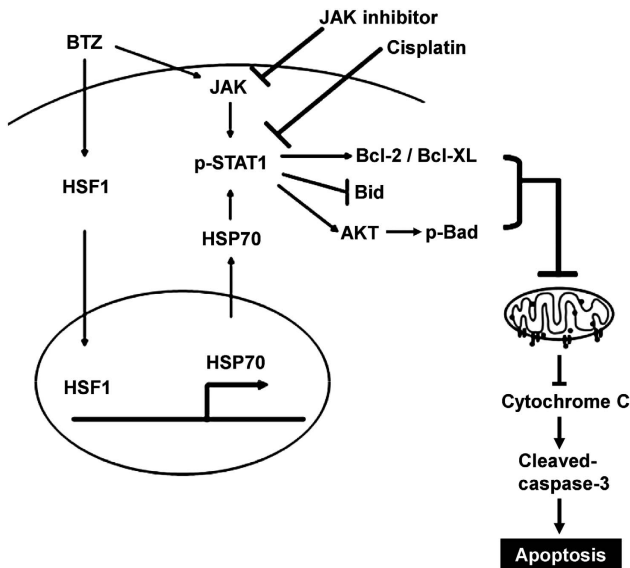


**Figure 7** The upregulation of HSP70 and the phosphorylation of STAT1 induced by bortezomib (BTZ) decrease the cytotoxic activity against ovarian cancer cells. BTZ increased HSF-1 and transcriptionally upregulated HSP70, which subsequently induced STAT1 phosphorylation. Moreover, BTZ can induce the phosphorylation of STAT1 through the JAK signaling pathway. Notably, cisplatin and JAKi I significantly inhibited STAT1 phosphorylation and enhanced cytotoxicity in BTZ-treated cells. These results suggest the possibility to abolish or reduce BTZ chemoresistance in ovarian cancer by the addition of cisplatin or JAKi's

pathways involved in cell cycle regulation (E2F1 and C/EBP), inflammation and cell migration (STATs, NF- $\kappa$ B, MMP-9, and HRE), cell proliferation (B23, YY1, Wnt pathway, ID3, and NF- $\kappa$ B), and stress-induced chaperone proteins (Grp78 and HSE (heat-shock factor response element)). Unexpectedly, we found that NF- $\kappa$ B transcription activity was not significantly affected by bortezomib (Figure 1e), although inhibition of the transcription factor NF- $\kappa$ B by bortezomib was thought to be a key molecular mechanism for antimyeloma.<sup>4</sup> Therefore, the transcription factor NF- $\kappa$ B does not seem to have a key role in the molecular mechanisms of bortezomib-mediated cytotoxicity in ovarian cancer cells. On the other hand, we have shown that bortezomib specifically promoted the tyrosine phosphorylation of STAT1, whereas a broad-spectrum proteasome inhibitor (MG132) did not (Figure 1f).

Dysregulation of STAT1 has been shown in many types of cancer,<sup>23</sup> but its roles can be either proapoptotic<sup>24</sup> or prosurvival.<sup>25,26</sup> STAT1 is significantly overexpressed in drug-resistant cancer cells compared with drug-sensitive cancer cells or normal cells.<sup>11</sup> The activation of the STAT1 signaling pathway has been shown to inhibit apoptosis in ovarian cancer<sup>12</sup> and is one of the molecular mechanisms underlying sarcoma development,<sup>27</sup> although exceptions exist.<sup>28</sup> The role of STAT1 in tumor biology and therapeutic resistance appears to differ from cell type to cell type. The results of this study indicate that an increased STAT1 phosphorylation was associated with a reduced sensitivity to bortezomib in ovarian cancer cell lines (Figure 1). We also demonstrated that the phosphorylation of STAT1 increased drug resistance (i.e., decreased cytotoxicity) in bortezomib-treated ovarian cancer cells (Figures 2, 4, and 5). Overexpression of an

S727E-substituted STAT1, which mimicks the constitutive phosphorylation of S727,<sup>29</sup> promoted cell viability and counteracted bortezomib-mediated cell death (Figure 2h and Supplementary Figure 5), further supporting this notion.

Bortezomib has been shown to induce apoptosis through the activation of proapoptotic proteins and/or the inhibition of antiapoptotic molecules.<sup>30,31</sup> The findings of this study are broadly consistent with earlier data obtained in bortezomib-treated ovarian cancer.<sup>16,32</sup> For example, previous research suggested that STAT1 may attenuate apoptosis<sup>33</sup> and enhance cancer cell growth.<sup>12</sup> Here, we show that STAT1 has a crucial role in the development of bortezomib resistance by promoting the expression of Bcl-2, Bcl-XL, and p-Bad (Figure 4). Interestingly, bortezomib increased the cleavage of Bid, as a part of apoptotic features, and knockdown of STAT1 enhanced the cleavage of Bid in bortezomib-treated cells (Figure 4c).

The upregulation of HSP70 observed in this study (Figure 3a) is part of the bortezomib-induced stress response, which was mediated by HSF (Figures 3g and h). In MM, the combination of bortezomib and CNTO 328, an anti-IL-6 monoclonal antibody, has been shown to decrease bortezomib-stimulated HSP70 and to inhibit STAT1 phosphorylation.<sup>34</sup> The results from this study demonstrate that the knockdown of HSP70 in bortezomib-treated cancer cells decreased STAT1 phosphorylation and increased apoptosis. In accordance with our working hypothesis (Figure 7), both the antiapoptotic HSP70 and STAT1 have been shown to be involved in the development of anticancer drug resistance.<sup>35–37</sup> It has been shown that JAK–STAT pathway activated HSP70 promoter via HSF-1 and increased levels of HSP70.<sup>35,38</sup> However, the mechanisms by which HSP70 mediates the phosphorylation of STAT1 remain to be determined.

In combination with bortezomib, inhibitors for JAK–STAT pathway have been used for anti-MM and leukemia therapies.<sup>39–41</sup> AG490 and JAKi I have been shown to decrease STAT phosphorylation and enhance cell death.<sup>12,42</sup> Although both AG490 and JAKi I alone were not sufficient to induce cell death in ovarian cancer cell lines, we found that their combination significantly inhibited bortezomib-induced STAT1 phosphorylation and enhanced the cytotoxic effects of bortezomib both *in vitro* and *in vivo* (Figures 2 and 6). These results support the potential usefulness of JAKi's and bortezomib combinations as a therapeutic strategy in ovarian cancer.

Bortezomib has been successfully used to overcome cisplatin resistance in ovarian cancer cells.<sup>43,44</sup> The synergistic effects of cisplatin and bortezomib have been explained by the removal of cisplatin resistance.<sup>45</sup> Alternatively, cisplatin may render the cells sensitive to bortezomib by modulating the STAT1 pathway, which is considered one of the major molecular mechanisms involved in cisplatin resistance.<sup>12,46</sup> Previous research also suggests that bortezomib may enhance cisplatin uptake and cytotoxicity by modulating the expression of the human copper transporter 1.<sup>47</sup> The results of this study demonstrate that subcytotoxic concentrations of cisplatin reduced bortezomib-induced STAT1 phosphorylation and enhanced the cytotoxic effects of bortezomib in ovarian cancer cells (Figure 5). Taken together, our data offer

an alternative mechanism to explain the synergistic cytotoxic effects of bortezomib and cisplatin.

In conclusion, we have shown that bortezomib may promote STAT1 phosphorylation in ovarian cancer cells through multiple signaling pathways. STAT1 phosphorylation can have a role in bortezomib resistance by exerting antiapoptotic effects. They also suggest the possibility to abolish or reduce bortezomib chemoresistance in ovarian cancer by the addition of cisplatin or JAK1's.

### Materials and Methods

**Cell culture and reagents.** Human ovarian cancer cell lines TOV112D, TOV21G, OVCAR3, OV90, SKOV3, MDAH2774, 67-R, and ES2 were obtained from ATCC (Rockville, MD, USA). BR and BG1 cells were obtained as described previously.<sup>48,49</sup> The cells were cultured in Dulbecco's modified Eagle's medium/F-12 supplemented with 10% fetal bovine serum and antibiotics at 37 °C in 5% CO<sub>2</sub> humidified atmosphere. OVCAR3 cells were cultured in RPMI 1640 media supplemented with 20% fetal bovine serum. Bortezomib (Millennium Pharmaceuticals, Cambridge, MA, USA) was dissolved in sterile water (final concentration: 10 mM). MG132 (Affinity Research Products Ltd, Exeter, UK), JAK1 I (Merck, Darmstadt, Germany), and paclitaxel (Sigma, St. Louis, MO, USA) were individually dissolved in DMSO (final concentration: 10 mM). The JAK2-specific inhibitor, AG490 (Merck), was dissolved in sterile water at a final concentration of 35 μM. Overexpression vectors for HSP70, HSF-1, and EGFP-STAT1 (S727E) were obtained from Addgene Inc. (Cambridge, MA, USA).

**Cell viability assay.** TOV112D cells were plated at 10 000 cells per well of 48-well plates. Cells were treated with the indicated concentrations of bortezomib in Dulbecco's modified Eagle's medium/F-12 supplemented with 10% fetal bovine serum for 24 h before being used in the assays. The inhibitory effects of bortezomib on the growth of tumor cells were measured by the MTT (3-(4,5-dimethylthiazol-2-yl)-2,5-diphenyltetrazolium bromide) method (Sigma). The optical density was measured at 570 nm using an automated scanning multiwell spectrophotometer (Wallac Victor2 spectrophotometer; Perkin-Elmer, Boston, MA, USA).

**Cell cytotoxicity assays.** The cytotoxicity of bortezomib was investigated using TOV112D and TOV21G cell lines. Cells were seeded at  $10^4$ – $2 \times 10^4$  cell per well of 96-well plates and treated with the aforementioned concentrations of bortezomib at 37 °C for 24 h. To calculate the activity of lactate dehydrogenase (LDH), 100 μl of a reaction mixture (Cytotoxicity Detection Kit PLUS; Roche, Basel, Switzerland) and the conditional medium were added to each well and incubated in the dark for 5–20 min. The water-soluble formazan dye exhibited the broad absorption maximum at approximately 500 nm in the Wallac Victor2 Spectrophotometer (Perkin-Elmer, Boston, MA, USA) Victor2 ELISA reader. The Cell Death Detection ELISA photometric enzyme immunoassay (Roche) was used for the quantitative *in vitro* determination of cytoplasmic histone-associated DNA fragments (mono- and oligonucleosomes) as an indicator of apoptosis. The absorbance was measured at 405 nm.

**Luciferase reporter assay.** C/EBP, E2F1, STATs (STAT1, STAT3, and STAT5), NF-κB, HRE, and HSE are response element luciferase reporter vectors. MMP-9, B23, ID3, YY1, TOP (TCF reporter gene), and Grp78 (HSPA5) are promoter luciferase reporter vectors. E2F1, NF-κB, MMP-9, B23, TOP, and Grp78 reporter vectors were obtained from Dr. Benjamin Yat-Ming Yung (Chang Gung University, Taiwan, Republic of China).<sup>50,51</sup> C/EBP, STATs, HSE, and YY1 reporter vectors were purchased from Panomics (Fremont, CA, USA). The HRE reporter vectors were obtained from Dr. Carine Michiels.<sup>52</sup> Two million cells were transfected by electroporation with 10 μg of each reporter plasmid DNA. We used a total of 10 reporter constructs (C/EBP, ID3, STAT1, TOP, Grp78, B23, HRE, MMP-9, E2F1, and YY1) and 1 μg of *Renilla* luciferase (Promega, Madison, WI, USA). The cells were then seeded at  $2 \times 10^3$  cells per well of 96-well plates and treated with bortezomib for 24 h. The luciferase activity was determined by a chemiluminescent assay reaction (Dual-Glo Luciferase Assay System; Promega). The *Renilla* luciferase expression was used to normalize for transfection efficiency.

**Western blot analysis.** The cells were lysed in ice-cold RIPA lysis buffer containing 1% Triton X-100, 1% NP-40, 0.1% SDS, 0.5% DOC, 20 mM

tris-hydroxymethyl-aminomethane (Tris-HCl, pH 7.4), 150 mM NaCl, and a mixture of protease and phosphatase inhibitors (Sigma) for 30 min. We used 10 and 12% resolving gels for separating proteins and identifying cleaved-caspase-3 by means of SDS-PAGE. The proteins were transferred to nitrocellulose membranes (Amersham Pharmacia Biotech, Uppsala, Sweden) and analyzed using the following primary antibodies: anti-HSP70 (K-20; Santa Cruz Biotechnology, Santa Cruz, CA, USA), anti-phospho-STAT1 (Tyr701), anti-phospho-STAT1 (Ser727), anti-STAT1, phospho-JAK1 (Tyr1022/1023), anti-JAK1, anti-cleaved-caspase-3 (Cell Signaling Technology, Beverly, MA, USA), and anti-HSF-1 (GeneTex, San Antonio, TX, USA). The reactions were probed with the corresponding horseradish peroxidase-conjugated secondary antibodies (Santa Cruz Biotechnology). The bands were subsequently developed with an enhanced chemiluminescence detection kit (ECL; Millipore, Bradford, MA, USA). To compare differences between samples, the relative intensity of each band was normalized to the intensity of the β-actin (Sigma) band amplified from the same sample.<sup>53</sup>

**Real-time quantitative PCR.** The mRNA level of the *HSP70* gene was measured in bortezomib-treated TOV112D cells lines. RNA was isolated using the Trizol reagent (Invitrogen, Carlsbad, CA, USA) according to the manufacturer's protocol.<sup>54</sup> Oligo(dT) primers were used in conjunction with the SuperScript III System (Invitrogen) for cDNA synthesis. The primer sequences for the human *HSP70* gene (*HSPA1B*) were 5'-ATTGAGGAGGTGGATTAG-3' (forward) and 5'-AGCGAAATGACATAGGA-3' (reverse). The amplification conditions were as follows: initial activation at 50 °C for 2 min and at 95 °C for 10 min, followed by 45 cycles at 95 °C for 15 s and 60 °C for 1 min using a thermal cycler system (MJ Research Inc., Waltham, MA, USA). The threshold cycle (C<sub>t</sub>) values were averaged from duplicate reactions.

**RNA interference.** For shRNA transfection experiments,  $2 \times 10^6$  cells were resuspended in 200 μl of RPMI 1640 and mixed with 30 μg of shRNA. Electroporation (100–120 V for 70 ms) was used to transfect shRNA on an ECM2001 instrument (BTX Instrument Division, Harvard Apparatus Inc., Holliston, MA, USA). The sequences of shRNA were as follows: 5'-CCGGCTTTGACAACAGCTGGTGAACCTCGAGTTCACCAGCCTGTTGTCAAAGTTTT-3' (HSP70); 5'-CCGGCCCTGAAAGTATCTGTATCCAACTCGAGTTGGATACAGATACTTCAGGGTTT-3' (STAT1); and 5'-CCGGGCAGGTTGTCATAGTCAGAACTCGAGTTCTGACTATGAACAACCTGCTTTTT-3' (HSF-1).

All of the sequences were provided by the National RNAi Core Facility, Academia Sinica (Taiwan, Republic of China).

**DNA transfection.** For HSP70 and HSF-1 overexpression,  $2 \times 10^6$  TOV112D cells were resuspended in 200 μl of RPMI 1640 and mixed with 20 μg of plasmid DNA expression vectors. Electroporation (100 V for 70 ms) was used to transfect plasmid DNA, as described above. The expression vectors corresponding to the human cDNA sequences for pEGFP-HSP70 and pBABE HSF Flag wt were purchased from Addgene Inc.

**Mice.** Female C57BL/6 mice (5 weeks old) were obtained from the National Animal Center (Taiwan, Republic of China). All of the procedures carried out in this study were approved by the Institutional Animal Care and Use Committee of the Chang Gung Memorial Hospital (no. 2008082602). All of the experiments conformed to the Guide for the Care and Use of Laboratory Animals published by the US National Institutes of Health (NIH Publication No.85-23, revised 1996).

**Tumor growth monitoring using an *in vivo* imaging system.** The dilution to 100 μl of  $10^7$  mouse ovarian surface epithelial cancer cells that constitutively expressed luciferase (MOSEC/LUC) was carried out by using Hank's balanced salt solution (HBSS). Mice were injected intraperitoneally using a 23-gauge needle (Becton Dickson, Franklin Lakes, NJ, USA). After 2–4 days, mice were injected with luciferin intraperitoneally (100 μl of 0.4 mg/ml luciferin; Promega) and imaged with an IVIS imaging system (Xenogen Corp.) 10 min after injection. All mice were sedated with isoflurane and imaged at the Molecular Imaging Core Laboratory of Chang Gung Memorial Hospital (Taiwan, Republic of China). Light outputs were quantified using the LivingImage software (Xenogen Corp.). Raw values were reported as photons/s/cm<sup>2</sup>/sr.

**Immunohistochemistry.** Paraffin-embedded tumor tissue sections (4 μm) were deparaffinized with xylene and rehydrated through an ethanol series. Sections were stained with an anticlaved-caspase-3 antibody (Cell Signaling

Technology) using an immunohistochemistry stainer equipped with a Ventana Basic DAB (3, 30-diaminobenzidine) Detection Kit (Tucson, AZ, USA) according to the manufacturer's protocol. Hematoxylin was used for counterstaining in all specimens.

**Immunofluorescent microscopy.** After transiently transfected with EGFP/EGFP-STAT1 (S727E), TOV112D cells were cultured on chamberslide at the concentration of  $10^3$  cells per well overnight. After being treated with bortezomib overnight, cells were fixed with acetone for 5 min and incubated in blocking buffer (5% normal goat serum in PBS) for 1 h at RT to reduce nonspecific binding. For cleaved-caspase-3 staining, cells were incubated with a rabbit polyclonal antibody (Cell Signaling; 1:100) overnight. After being incubated with anti-rabbit Alexa Fluor 546 (1:100; Invitrogen), the slides were mounted with VECTASHIELD mounting medium (Vector Laboratories, Burlingame, CA, USA), and analyzed with the Leica TCS SP2 laser-scanning confocal system (Leica, Mannheim, Germany).

**Data analysis.** All of the data are expressed as mean  $\pm$  standard error of the mean, unless otherwise indicated. The results are representative of at least three independent experiments. Group comparisons were performed using two-tailed *t*-tests with the SPSS statistical software (Version 17; SPSS Inc., Chicago, IL, USA). Two-tailed *P*-values  $<0.05$  were considered statistically significant.

### Conflict of Interest

The authors declare no conflict of interest.

**Acknowledgements.** We are grateful to Dr. Kowit-Yu Chong (Chang Gung University) for helpful discussions. We also thank the Microscopy Core Laboratory (Chang Gung Memorial Hospital) for the help with the confocal images and the Animal Molecular Imaging Center (Chang Gung Memorial Hospital) for the help with the IVIS study. These results were presented in part at the '68th Harden – Autophagy: from molecules to disease' conference, which took place on 8–12 September 2010 (Royal Agricultural College, Gloucestershire, UK). This study was supported by grants from the National Science Council of Taiwan (NSC100-2314-B-182-016-MY3 to THW), the Chang Gung Medical Research Foundation (CMRPG391452 to AC, and CMRPG391461 and CMRPG 360914 to THW), and the Department of Health of Taiwan (DOH99-TD-I-111-TM013 to THW, and DOH99-TD-C-111-006 to AC and THW).

### Author contributions

CK, CLT, CYL, WCC, and HWC performed the experiments. CK, AC, THW, TCY, CHL, and HSW designed the study and analyzed the data. CK, AC, and THW wrote the manuscript.

- Richardson PG, Barlogie B, Berenson J, Singhal S, Jagannath S, Irwin D *et al*. A phase 2 study of bortezomib in relapsed, refractory myeloma. *N Engl J Med* 2003; **348**: 2609–2617.
- Baritaki S, Suzuki E, Umezawa K, Spandidos DA, Berenson J, Daniels TR *et al*. Inhibition of Yin Yang 1-dependent repressor activity of DR5 transcription and expression by the novel proteasome inhibitor NPI-0052 contributes to its TRAIL-enhanced apoptosis in cancer cells. *J Immunol* 2008; **180**: 6199–6210.
- Pandit B, Gartel AL. Proteasome inhibitors suppress expression of NPM and ARF proteins. *Cell Cycle* 2011; **10**: 3827–3829.
- Paramore A, Frantz S. Bortezomib. *Nat Rev Drug Discov* 2003; **2**: 611–612.
- Beg AA, Baltimore D. An essential role for NF-kappaB in preventing TNF-alpha-induced cell death. *Science* 1996; **274**: 782–784.
- Berenson JR, Yang HH, Sadler K, Jarutirasam SG, Vescio RA, Mapes R *et al*. Phase I/II trial assessing bortezomib and melphalan combination therapy for the treatment of patients with relapsed or refractory multiple myeloma. *J Clin Oncol* 2006; **24**: 937–944.
- Barlogie B, Shaughnessy J, Tricot G, Jacobson J, Zangari M, Anaissie E *et al*. Treatment of multiple myeloma. *Blood* 2004; **103**: 20–32.
- Sironi JJ, Ouchi T. STAT1-induced apoptosis is mediated by caspases 2, 3, and 7. *J Biol Chem* 2004; **279**: 4066–4074.
- Vilcek J. Novel interferons. *Nat Immunol* 2003; **4**: 8–9.
- Chang CW, Tsai WH, Chuang WJ, Lin YS, Wu JJ, Liu CC *et al*. Procaspase 8 and Bax are up-regulated by distinct pathways in Streptococcal pyrogenic exotoxin B-induced apoptosis. *J Biol Chem* 2009; **284**: 33195–33205.
- Perou CM, Jeffrey SS, van de Rijn M, Rees CA, Eisen MB, Ross DT *et al*. Distinctive gene expression patterns in human mammary epithelial cells and breast cancers. *Proc Natl Acad Sci USA* 1999; **96**: 9212–9217.
- Roberts D, Schick J, Conway S, Biade S, Laub PB, Stevenson JP *et al*. Identification of genes associated with platinum drug sensitivity and resistance in human ovarian cancer cells. *Br J Cancer* 2005; **92**: 1149–1158.
- Siegel R, Naishadham D, Jemal A. Cancer statistics 2012. *CA Cancer J Clin* 2012; **62**: 10–29.
- McGuire WP, Hoskins WJ, Brady MF, Kucera PR, Partridge EE, Look KY *et al*. Cyclophosphamide and cisplatin compared with paclitaxel and cisplatin in patients with stage III and stage IV ovarian cancer. *N Engl J Med* 1996; **334**: 1–6.
- Greenlee RT, Hill-Harmon MB, Murray T, Thun M. Cancer statistics 2001. *CA Cancer J Clin* 2001; **51**: 15–36.
- Bazzaro M, Lee MK, Zoso A, Stirling WL, Santillan A, Shih IM *et al*. Ubiquitin–proteasome system stress sensitizes ovarian cancer to proteasome inhibitor-induced apoptosis. *Cancer Res* 2006; **66**: 3754–3763.
- Aghajanian C, Dizon DS, Sabbatini P, Raizer JJ, Dupont J, Spriggs DR. Phase I trial of bortezomib and carboplatin in recurrent ovarian or primary peritoneal cancer. *J Clin Oncol* 2005; **23**: 5943–5949.
- Frankel A, Man S, Elliott P, Adams J, Kerbel RS. Lack of multicellular drug resistance observed in human ovarian and prostate carcinoma treated with the proteasome inhibitor PS-341. *Clin Cancer Res* 2000; **6**: 3719–3728.
- Aghajanian C, Blessing JA, Darcy KM, Reid G, DeGeest K, Rubin SC *et al*. A phase II evaluation of bortezomib in the treatment of recurrent platinum-sensitive ovarian or primary peritoneal cancer: a Gynecologic Oncology Group study. *Gynecol Oncol* 2009; **115**: 215–220.
- Powers MV, Clarke PA, Workman P. Dual targeting of HSC70 and HSP72 inhibits HSP90 function and induces tumor-specific apoptosis. *Cancer Cell* 2008; **14**: 250–262.
- NCI Guidelines for Investigators: Adverse Event Reporting Requirements for DCTD(CTEP and CIP) and DCPINDs and IDE 2012 1–35.
- ClinicalTrials.gov <http://clinicaltrials.gov/ct2/home> 2012.
- Bowman T, Garcia R, Turkson J, Jove R. STATs in oncogenesis. *Oncogene* 2000; **19**: 2474–2488.
- Kaplan DH, Shankaran V, Dighe AS, Stockert E, Aguet M, Old LJ *et al*. Demonstration of an interferon gamma-dependent tumor surveillance system in immunocompetent mice. *Proc Natl Acad Sci USA* 1998; **95**: 7556–7561.
- Carlesso N, Frank DA, Griffin JD. Tyrosyl phosphorylation and DNA binding activity of signal transducers and activators of transcription (STAT) proteins in hematopoietic cell lines transformed by Bcr/Abl. *J Exp Med* 1996; **183**: 811–820.
- Frank DA, Mahajan S, Ritz J. B lymphocytes from patients with chronic lymphocytic leukemia contain signal transducer and activator of transcription (STAT) 1 and STAT3 constitutively phosphorylated on serine residues. *J Clin Invest* 1997; **100**: 3140–3148.
- Zimmerman MA, Rahman NT, Yang D, Lahat G, Lazar AJ, Pollock RE *et al*. Unphosphorylated STAT1 promotes sarcoma development through repressing expression of Fas and bad and conferring apoptotic resistance. *Cancer Res* 2012; **72**: 4724–4732.
- Dimberg LY, Dimberg A, Ivarsson K, Fryknas M, Rickardson L, Tobin G *et al*. Stat1 activation attenuates IL-6 induced Stat3 activity but does not alter apoptosis sensitivity in multiple myeloma. *BMC Cancer* 2012; **12**: 318.
- Timofeeva OA, Plisov S, Evseev AA, Peng S, Jose-Kampfner M, Lovorn HN *et al*. Serine-phosphorylated STAT1 is a prosurvival factor in Wilms' tumor pathogenesis. *Oncogene* 2006; **25**: 7555–7564.
- Yeung BH, Huang DC, Sinicrope FA. PS-341 (bortezomib) induces lysosomal cathepsin B release and a caspase-2-dependent mitochondrial permeabilization and apoptosis in human pancreatic cancer cells. *J Biol Chem* 2006; **281**: 11923–11932.
- Wolter KG, Verhaegen M, Fernandez Y, Nikolovska-Coleska Z, Riblett M, de la Vega CM *et al*. Therapeutic window for melanoma treatment provided by selective effects of the proteasome on Bcl-2 proteins. *Cell Death Differ* 2007; **14**: 1605–1616.
- Saule E, Petronelli A, Pasquini L, Petrucci E, Mariani G, Biffoni M *et al*. Proteasome inhibitors sensitize ovarian cancer cells to TRAIL induced apoptosis. *Apoptosis* 2007; **12**: 635–655.
- Hsu WL, Chiu TH, Tai DJ, Ma YL, Lee EH. A novel defense mechanism that is activated on amyloid-beta insult to mediate cell survival: role of SGK1-STAT1/STAT2 signaling. *Cell Death Differ* 2009; **16**: 1515–1529.
- Voorhees PM, Chen Q, Kuhn DJ, Small GW, Hunsucker SA, Strader JS *et al*. Inhibition of interleukin-6 signaling with CNTO 328 enhances the activity of bortezomib in preclinical models of multiple myeloma. *Clin Cancer Res* 2007; **13**: 6469–6478.
- Stephanou A, Isenberg DA, Nakajima K, Latchman DS. Signal transducer and activator of transcription-1 and heat shock factor-1 interact and activate the transcription of the Hsp-70 and Hsp-90beta gene promoters. *J Biol Chem* 1999; **274**: 1723–1728.
- Madamanchi NR, Li S, Patterson C, Runge MS. Thrombin regulates vascular smooth muscle cell growth and heat shock proteins via the JAK-STAT pathway. *J Biol Chem* 2001; **276**: 18915–18924.
- Salvioli S, Storci G, Pinti M, Quaglino D, Moretti L, Merlo-Pich M *et al*. Apoptosis-resistant phenotype in HL-60-derived cells HCW-2 is related to changes in expression of stress-induced proteins that impact on redox status and mitochondrial metabolism. *Cell Death Differ* 2003; **10**: 163–174.
- Madamanchi NR, Li S, Patterson C, Runge MS. Reactive oxygen species regulate heat-shock protein 70 via the JAK/STAT pathway. *Arterioscler Thromb Vasc Biol* 2001; **21**: 321–326.

39. Monaghan KA, Khong T, Burns CJ, Spencer A. The novel JAK inhibitor CYT387 suppresses multiple signalling pathways, prevents proliferation and induces apoptosis in phenotypically diverse myeloma cells. *Leukemia* 2011; **25**: 1891–1899.
40. Pham LV, Tamayo AT, Li C, Bornmann W, Priebe W, Ford RJ. Degrasyn potentiates the antitumor effects of bortezomib in mantle cell lymphoma cells *in vitro* and *in vivo*: therapeutic implications. *Mol Cancer Ther* 2010; **9**: 2026–2036.
41. Park J, Ahn KS, Bae EK, Kim BS, Kim BK, Lee YY *et al*. Blockage of interleukin-6 signaling with 6-amino-4-quinazoline synergistically induces the inhibitory effect of bortezomib in human U266 cells. *Anticancer Drugs* 2008; **19**: 777–782.
42. Cochet O, Frelin C, Peyron JF, Imbert V. Constitutive activation of STAT proteins in the HDLM-2 and L540 Hodgkin lymphoma-derived cell lines supports cell survival. *Cell Signal* 2006; **18**: 449–455.
43. Al-Eisawi Z, Beale P, Chan C, Yu JQ, Huq F. Modulation of cisplatin cytotoxicity due to its combination with bortezomib and the nature of its administration. *Anticancer Res* 2011; **31**: 2757–2762.
44. Pasquini L, Petronelli A, Petrucci E, Saulle E, Mariani G, Scambia G *et al*. Primary ovarian cancer cells are sensitive to the proapoptotic effects of proteasome inhibitors. *Int J Oncol* 2010; **36**: 707–713.
45. Fribley AM, Evenchik B, Zeng Q, Park BK, Guan JY, Zhang H *et al*. Proteasome inhibitor PS-341 induces apoptosis in cisplatin-resistant squamous cell carcinoma cells by induction of Noxa. *J Biol Chem* 2006; **281**: 31440–31447.
46. Stronach EA, Alfraidi A, Rama N, Datler C, Studd JB, Agarwal R *et al*. HDAC4-regulated STAT1 activation mediates platinum resistance in ovarian cancer. *Cancer Res* 2011; **71**: 4412–4422.
47. Jandial DD, Farshchi-Heydari S, Larson CA, Elliott GI, Wrasidlo WJ, Howell SB. Enhanced delivery of cisplatin to intraperitoneal ovarian carcinomas mediated by the effects of bortezomib on the human copper transporter 1. *Clin Cancer Res* 2009; **15**: 553–560.
48. Guo HF, Su HL, Mao JJ, Sun C, Wang J, Zhou X. Stroke after treatment with bortezomib and dexamethasone in a Chinese patient with extramedullary relapse of multiple myeloma. *Int J Clin Pharmacol Ther* 2010; **48**: 776–778.
49. Wang TH, Wang HS, Ichijo H, Giannakakou P, Foster JS, Fojo T *et al*. Microtubule-interfering agents activate c-Jun N-terminal kinase/stress-activated protein kinase through both Ras and apoptosis signal-regulating kinase pathways. *J Biol Chem* 1998; **273**: 4928–4936.
50. Lin CY, Liang YC, Yung BY. Nucleophosmin/B23 regulates transcriptional activation of E2F1 via modulating the promoter binding of NF-kappaB, E2F1 and pRB. *Cell Signal* 2006; **18**: 2041–2048.
51. Yeh CW, Huang SS, Lee RP, Yung BY. Ras-dependent recruitment of c-Myc for transcriptional activation of nucleophosmin/B23 in highly malignant U1 bladder cancer cells. *Mol Pharmacol* 2006; **70**: 1443–1453.
52. Michiels C. Physiological and pathological responses to hypoxia. *Am J Pathol* 2004; **164**: 1875–1882.
53. Chao A, Tsai CL, Wei PC, Hsueh S, Chao AS, Wang CJ *et al*. Decreased expression of microRNA-199b increases protein levels of SET (protein phosphatase 2A inhibitor) in human choriocarcinoma. *Cancer Lett* 2010; **291**: 99–107.
54. Chao A, Wang TH, Lee YS, Hsueh S, Chao AS, Chang TC *et al*. Molecular characterization of adenocarcinoma and squamous carcinoma of the uterine cervix using microarray analysis of gene expression. *Int J Cancer* 2006; **119**: 91–98.



**Cell Death and Disease** is an open-access journal published by Nature Publishing Group. This work is licensed under the Creative Commons Attribution-NonCommercial-No Derivative Works 3.0 Unported License. To view a copy of this license, visit <http://creativecommons.org/licenses/by-nc-nd/3.0/>

Supplementary Information accompanies the paper on Cell Death and Disease website (<http://www.nature.com/cddis>)